Deep Learning–Based Spatial Analysis of TLSs in CRC Reveals Stromal Barriers Predicting Impaired Cell–Cell Communication

Amina Nurmammadova*[1], Yu Ding*[2], Afrooz Jahedi[3], Mesut Unal[4], Yunhe Liu[3], Linghua Wang[3], Garry P. Nolan[6]

Departments of Cell Therapy Discovery and Innovation[1], Bioinformatics and Computation Biology[2] ,Genomic Medicine[3], Neurosurgery[4], at the University of Texas MD Anderson Cancer Center, Houston, TX, USA and Department of Pathology at the Stanford University School of Medicine[5], CA, USA

THE UNIVERSITY OF TEXAS MD Anderson Cancer Center
Making Cancer History®

James P. Allison Institute

INSTITUTE FOR DATA SCIENCE IN ONCOLOGY

Introduction

Colorectal cancer (CRC) treatment remains challenging due to high rates of therapeutic resistance and relapse, underscoring the urgent need to decode resistance. Immunotherapy has transformed oncology, yet only a fraction of CRC patients derive benefit. The immune tumor microenvironment (iTME) is spatially organized in ways that critically shape antitumor immunity and therapy response. Tertiary lymphoid structures (TLS) have emerged as key prognostic correlates in many cancers, highlighting how local cell–cell interactions, both inside and outside TLS niches, may govern sensitivity or resistance to immunotherapies

Aim of the Study

This study aims to characterize the spatiotemporal organization of cells within TLSs in CRC patients treated with immune checkpoint inhibitors (ICIs) and to elucidate how stromal and immune cell interactions influence TLS formation, immune cell infiltration, and ultimately therapeutic response.

Methods

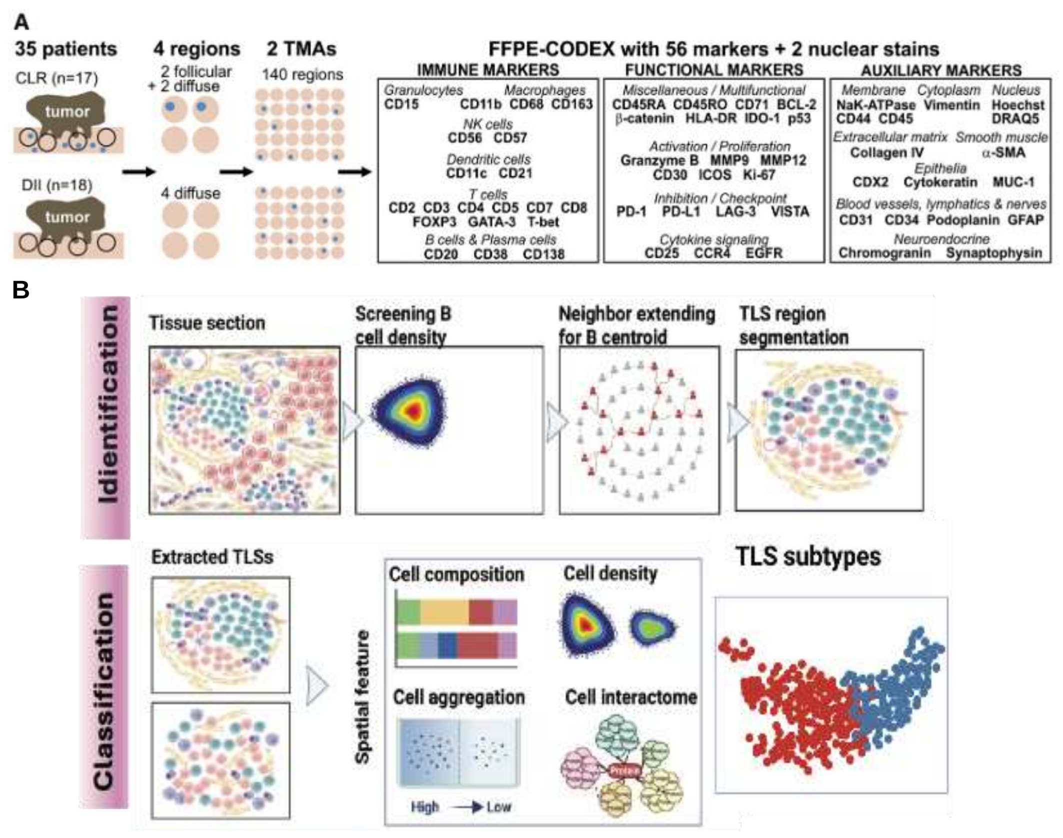

Figure 1. (A) Schematic representation of CRC tissue microarray (TMA) assembly. Blue dots indicate lymphoid follicles corresponding to TLSs. The analysis incorporated a panel of 58 antibody markers and 2 nuclear stains to annotate and classify diverse immune, stromal, and tumor cell populations[3]. **(B)** Workflow for TLS detection and classification. TLS regions were identified by mapping high B-cell density, expanding neighborhoods around B-cell centroids, and segmenting contiguous clusters. Extracted TLSs were characterized by cellular density, composition, aggregation, and intercellular network features.

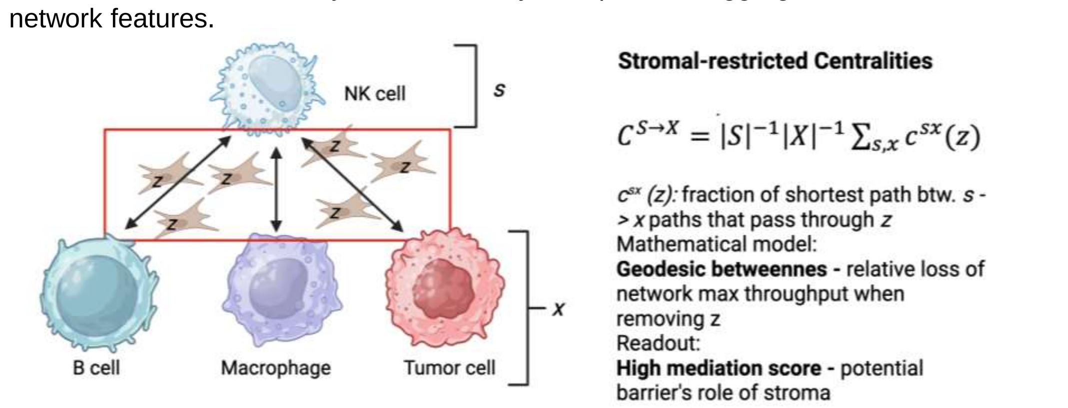

Figure 2. Stromal-restricted centralities model Stromal-restricted centrality analysis showing how stromal cells mediate immune-tumor communication. High mediation scores indicate a potential stromal barrier limiting immune infiltration.

References

[1]**Heregger R**, Huemer F, Steiner M, Gonzalez-Martinez A, Greil R, Weiss L. Unraveling Resistance to Immunotherapy in MSI-High Colorectal Cancer. ***Cancers***. 2023; 15(20):5090.

[2]**Sautès-Fridman, C**., Petitprez, F., Calderaro, J. *et al.* Tertiary lymphoid structures in the era of cancer immunotherapy. *Nat Rev Cancer* **19**, 307–325 (2019).

[3] **Schürch, C.M.,** Bhate, S.S., Barlow, G.L., et al. *Coordinated cellular neighborhoods orchestrate antitumoral immunity at the colorectal cancer invasive front.* ***Cell*** 182, 1341–1359.e19 (2020)

Results

Distinct cellular organization within and outside TLSs reflects differences in TLS maturation

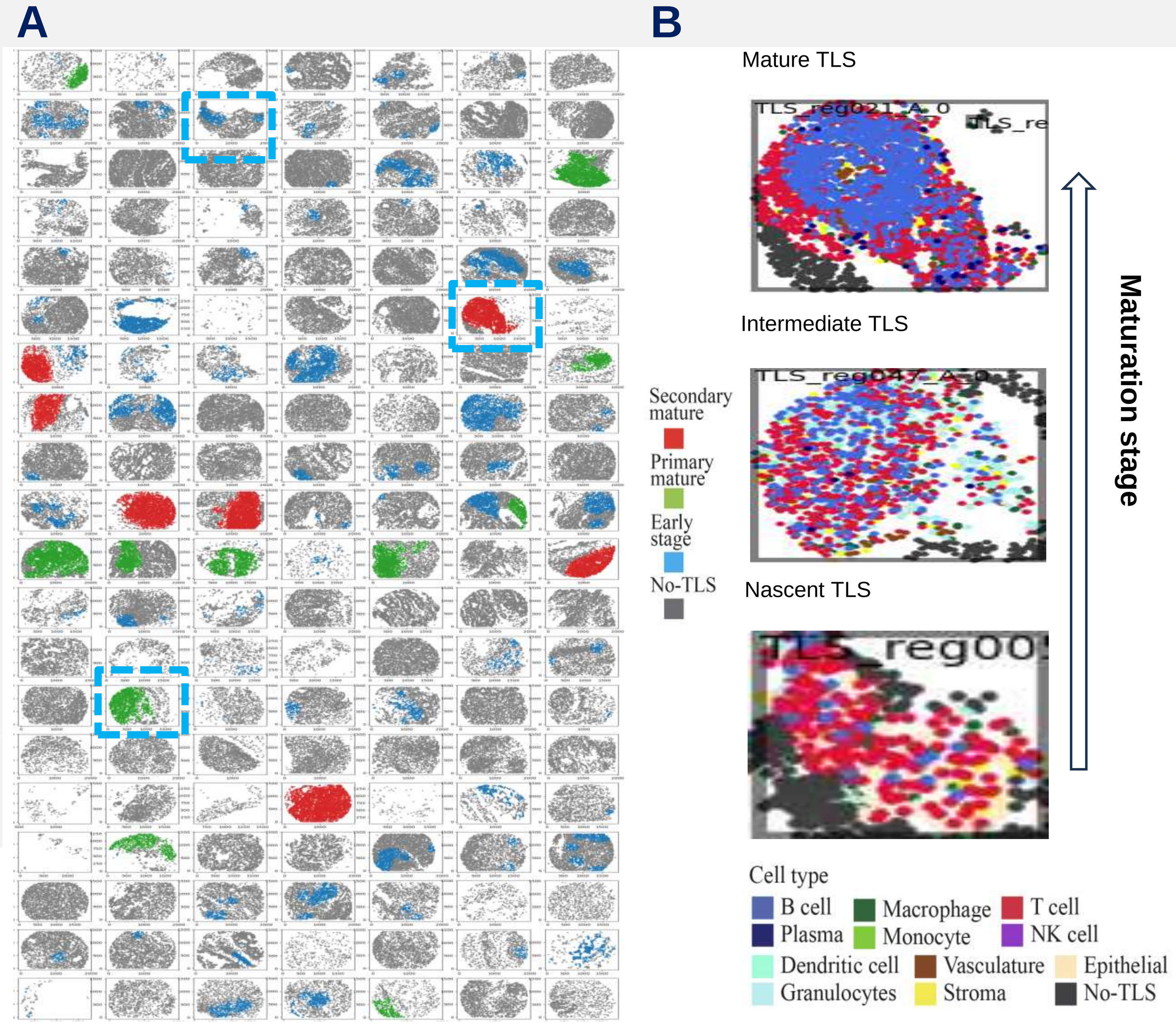

FIG 3. (A) Representative TLSs across TMA cohorts A and B illustrate classification into nascent (blue), intermediate (green), and mature (red) maturation states. **(B)** Cell composition derived by the classification algorithm provides reference distributions of immune subsets across TLS subtypes.

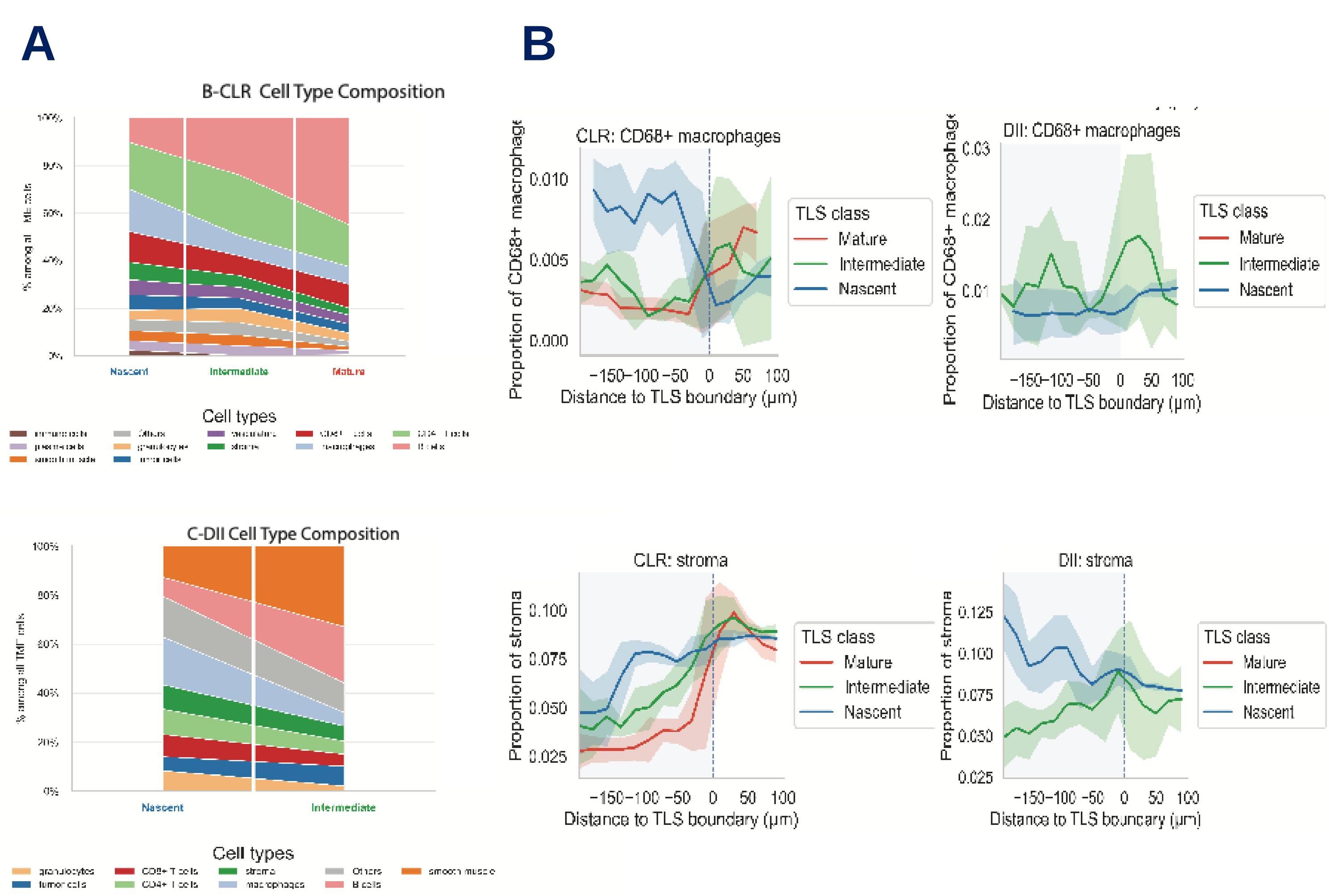

Fig. 4. (A) Cell type composition shifts across TLS maturation in CLR and DII patients. Combined analysis of CLR and DII TLSs shows significant changes in cell type proportions with maturation: decreased B and CD4⁺ T cells and increased plasma cells, macrophages, stroma, and tumor cells.
(B) Comparative spatial gradients of stroma, vasculature, and macrophages in CLR and DII TLSs. Line plots show proportions of stromal cells, CD68⁺ macrophages as a function of distance to TLS boundaries (negative = inside, positive=outside) across TLS maturation stages.

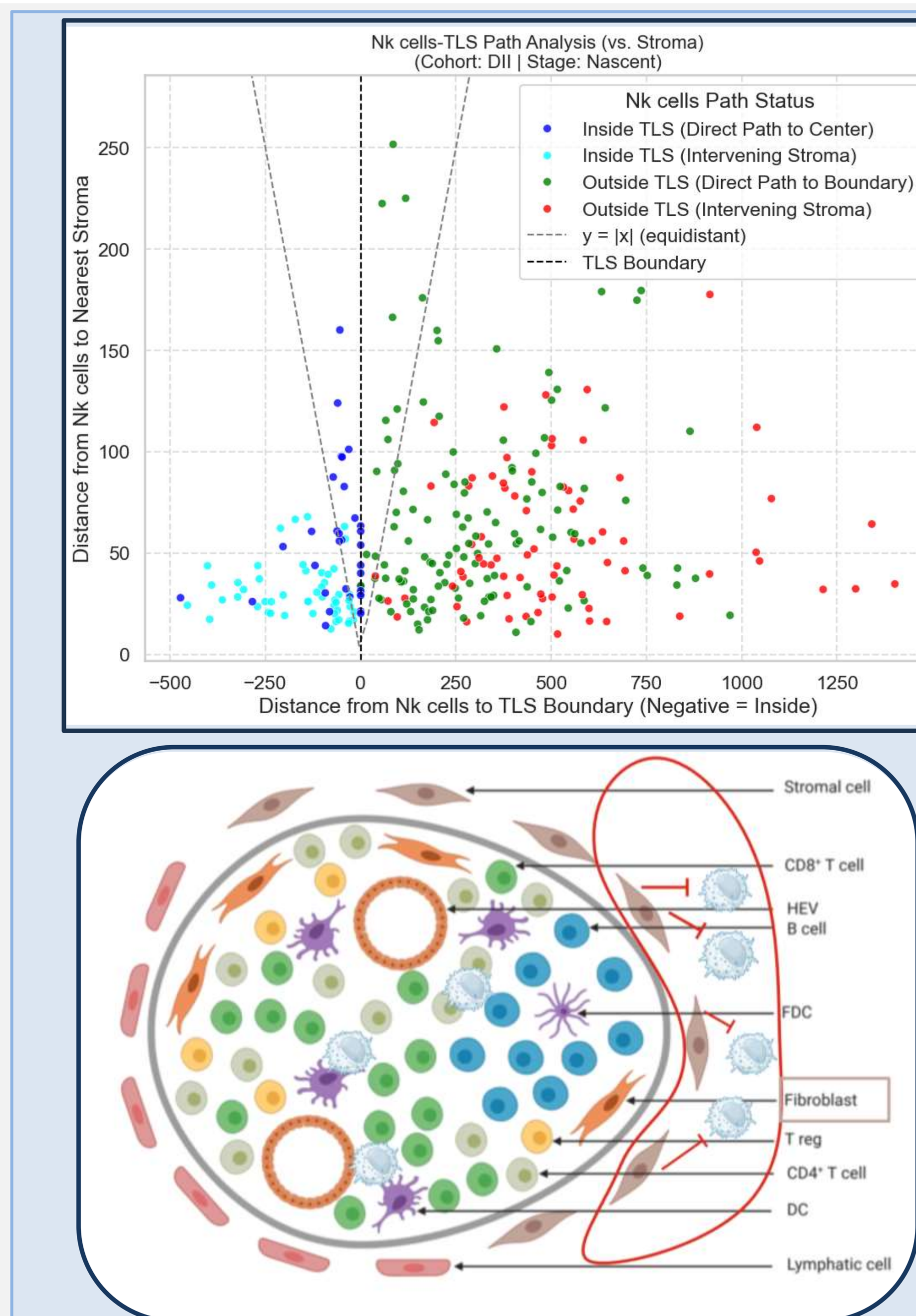

FIG 6. (A)NK cell–TLS path analysis relative to stromal barriers. Scatter plot showing distances of NK cells from the TLS boundary (x-axis) and from the nearest stromal cell (y-axis) in DII nascent TLSs. NK cells were classified based on path status: direct or stroma-intervened, either inside or outside TLS regions. Cells with intervening stroma exhibit increased distance to TLS centers or boundaries, suggesting stromal obstruction of NK infiltration. **(B) Proposed model of stromal-mediated blockade of NK cell infiltration into TLSs.** Schematic illustrating how fibroblast-rich stromal regions at the TLS periphery may hinder NK cell entry and interaction with intratumoral immune populations

Distinct NK cell distribution inside and outside TLSs reveals stromal interference with immune interactions

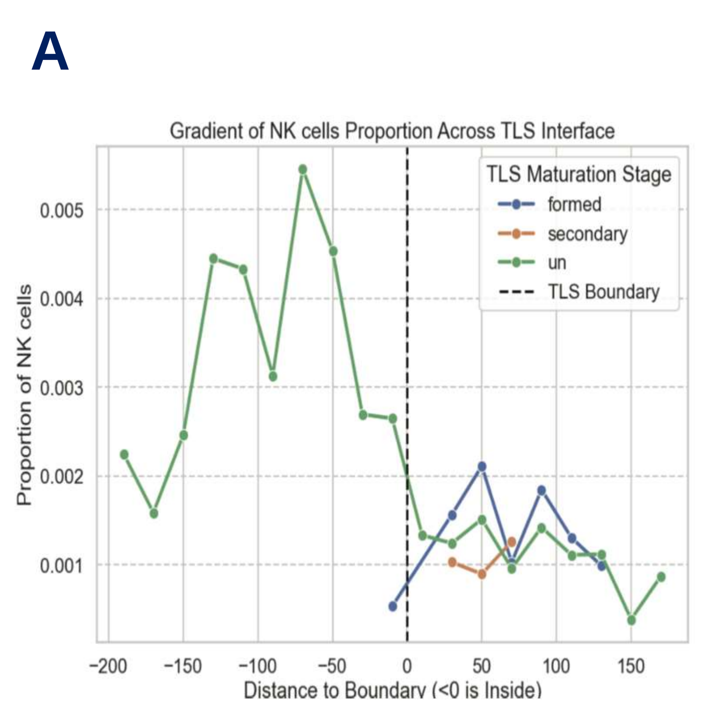

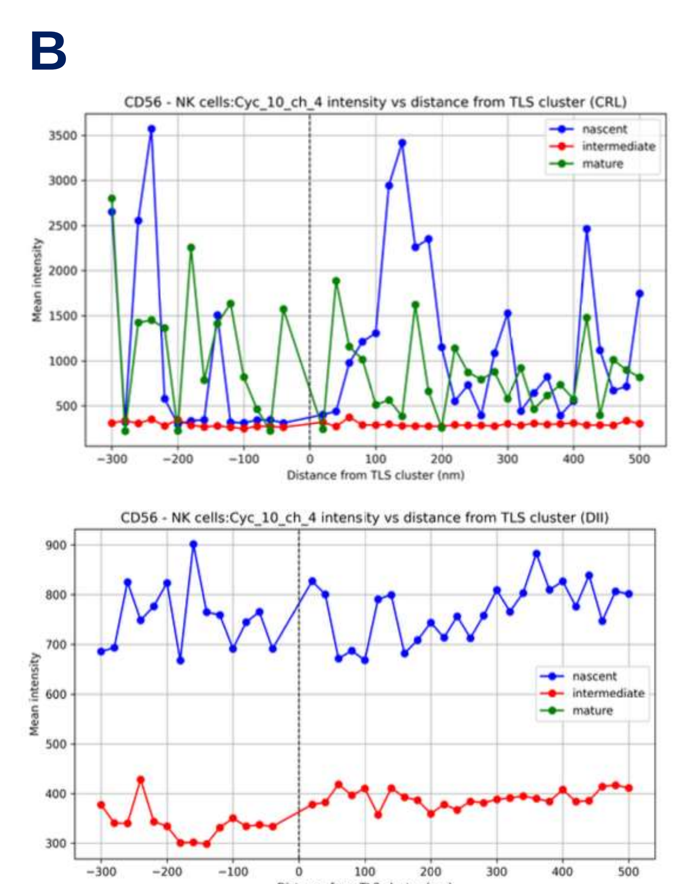

FIG 5. (A) Gradient of NK cell proportion across the TLS interface. The proportion of NK cells was quantified relative to the TLS boundary (dashed line) across different TLS maturation stages: unorganized (green), secondary (orange), and fully formed (blue). NK cells were more enriched outside immature TLSs, whereas mature TLSs showed a more balanced distribution across the boundary.
(B) NK cell mean intensity in CLR vs DII patients relative to the TLS boundary. NK cell signal intensity was highest near nascent and mature TLSs, suggesting dynamic NK localization and potential modulation by TLS maturation state within the CLR subtype. NK cell signal remained higher in nascent TLS regions, indicating limited NK enrichment near mature TLSs within the DII subtype

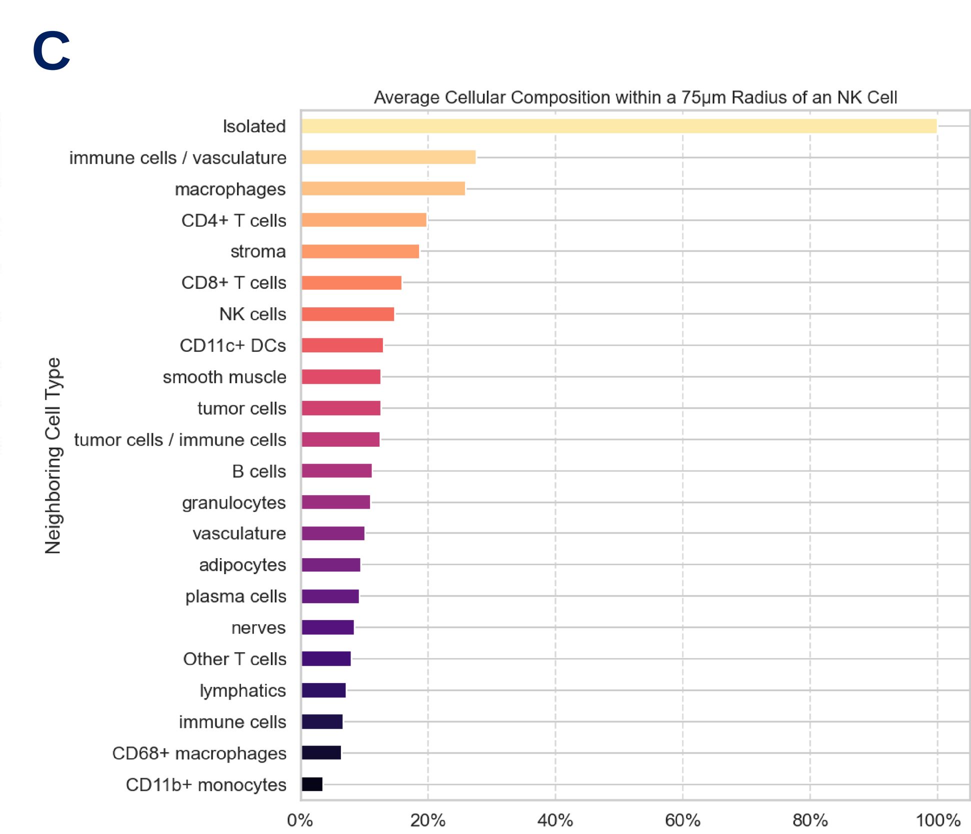

FIG 5. (C) Average neighborhood composition of NK cells. Bar plot showing the mean proportion of neighboring cell types within a 75 µm radius around NK cells. NK cells were frequently found near macrophages, CD4⁺ T cells, and stromal elements, though many remained spatially isolated, suggesting restricted immune connectivity.

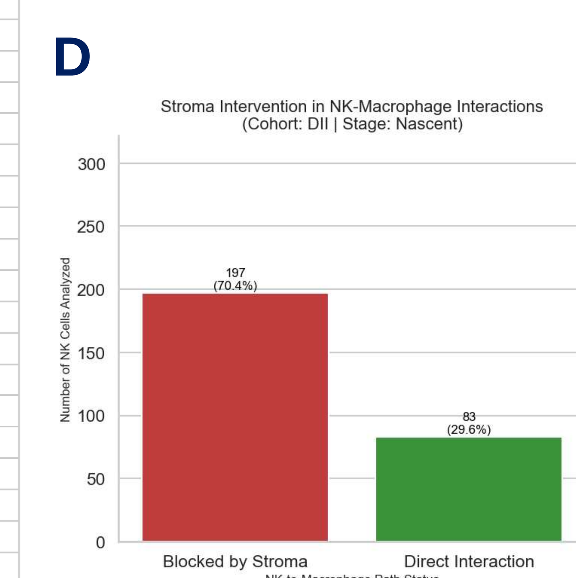

FIG 5. (D) Stromal interference in NK–macrophage interactions within DII nascent TLSs. Bar plot showing the proportion of NK cells whose communication paths to macrophages were either blocked by stromal cells (70.4%) or direct (29.6%).

Conclusions

- **Spatial modeling of TLS architecture revealed that the degree of stromal interference correlates with TLS formation and maturation.**
- **Stromal barriers play a key role in limiting immune cell infiltration and cell–cell communication within TLSs, particularly hindering NK-macrophage interactions in the DII subtype of CRC.**

Future Directions

Focus on identifying molecular and spatial cues within the stroma that regulate TLS formation and modulate immune cell infiltration to guide strategies enhancing immunotherapy efficacy.

Acknowledgments

To the patients and their families. This work was supported by the Institute of Data Science in Oncology and James P. Allison at the MD Anderson Cancer Center.

Contact

Amina Nurmammadova
LinkedIn: www.linkedin.com/in/amina-nurmammadova
ANurmammadova@mdanderson.org